

DOING PHYSICS WITH MATLAB

RAYLEIGH-SOMMERFELD DIFFRACTION INTEGRAL OF THE FIRST KIND

THE THREE-DIMENSIONAL DISTRIBUTION OF THE RADIANT FLUX DENSITY AT THE FOCUS OF A CONVERGENT BEAM

Ian Cooper

Please email any corrections, comments, suggestions or

additions: matlabvisualphysics@gmail.com

[Matlab Download Directory](#)

It is necessary to modify the mscripts and comment or uncomment lines of code to run the simulations with different input and output parameters.

op_rs_fb_xy.m

Calculation of the radiant flux density (irradiance) in a plane perpendicular to the optical axis for the radiant flux of convergent beam emitted from a circular aperture. It uses Method 3: one-dimensional form of Simpson's rule for the integration of the diffraction integral. This mscript is only valid for irradiance distributions that are circularly symmetrical about the optical axis (Z axis).

op_rs_fb_z.m

Calculation of the radiant flux density (irradiance) along the optical axis for the radiant flux of convergent beams emitted from a circular aperture. It uses Method 3: one-dimensional form of Simpson's rule for the integration of the diffraction integral.

op_rs_fb_xz.m

Calculation of the irradiance in the meridional - XZ plane for the radiant flux of convergent beam emitted from a circular aperture. It uses Method 3: one-dimensional form of Simpson's rule for the integration of the diffraction integral.

op_rs_fb_xyyz.m

Calculation of the radiant flux density (irradiance) in plane perpendicular to the optical axis for the radiant flux of a convergent beam emitted from a circular aperture for non-symmetrical cases and calculates the irradiance along the optical axis. It uses Method 3: one-dimensional form of Simpson's rule for the integration of the diffraction integral. This mscript runs slower than the other scripts as you can't make use of the circular symmetry when the source can be located off-axis.

Function calls to:

simpson1d.m (integration)

fn_distancePQ.m (calculates the distance between points P and Q)

turningPoints.m (finds the location of zeros, min and max of a function)

Warning: The results of the integration may look OK but they may not be accurate if you have used insufficient number of partitions for the aperture space and observation space. It is best to check the convergence of the results as the number partitions is increased. Note: as the number of partitions increases, the calculation time **rapidly** increases.

RAYLEIGH-SOMMERFELD DIFFRACTION INTEGRAL OF THE FIRST KIND

The Rayleigh-Sommerfeld diffraction integral of the first kind states that the electric field E_P at an observation point P can be expressed as

$$(1) \quad E_P = \frac{1}{2\pi} \iint_{S_A} E(\vec{r}) \frac{e^{jk r}}{r^3} z_p (j k r - 1) dS \quad \text{planar aperture space}$$

It is assumed that the Rayleigh-Sommerfeld diffraction integral of the first kind is valid throughout the space in front of the aperture, right down to the aperture itself. There are no limitations on the maximum size of either the aperture or observation region, relative to the observation distance, because **no approximations have been made**.

The diffraction pattern can be given in terms of the irradiance distribution w_e

$$(2) \quad w_e = \frac{n \varepsilon_0 c}{2} E_P^* E_P$$

where ε_0 is the permittivity of free space, c is the speed of light in vacuum, n is the refractive index of the medium and E_P is the peak value of the electric field at a point P in the observation space.

The time rate of flow of radiant energy is the **radiant flux** W_E where

$$(3) \quad W_E = \iint_{\text{area}} w_e dA$$

S.I. UNITS

Quantity	S.I. unit
distances	m
electric field	V.m ⁻¹
speed of light	m.s ⁻¹
permittivity of free space	C ² .N ⁻¹ .m ⁻²
irradiance, radiant flux density	W.m ⁻²
time rate of radiance energy, radiant flux	W or J.s ⁻¹

IMAGE FORMATION AND ITS RELATIONSHIP TO DIFFRACTION AND ABERRATIONS

The scalar theory of diffraction can be used to describe the formation of images and to account for the effects of aberrations that distort the image. Knowledge of the irradiance near the focal region is important for the performance of microscopes, telescopes and the focussing of lasers.

In a Gaussian image forming system, light from an object is focused by a lens to form an image of the object. In this geometrical optics approach, light from each point on the object is focused to a point in the image plane. However, due to the finite size of the lens and aberration effects, the light from a point on the object can't be focused to a point in the image plane. The image from each point on the object is smeared out reducing the resolution and degrading the quality of the image of the object.

It is possible to calculate the three-dimensional radiant flux density (irradiance) pattern in the image (observation) space for the light coming from a point source object. This calculation provides details of the smearing out of the image of the point source. This calculation forms part of the Abney theory of image formation, where the electric field in the image space is found using the Fresnel-Kirchhoff diffraction integral. But many approximations and much algebra are needed to find the electric field and the results are only applicable to special situations.

A much easier way to calculate the electric field in the image space and without all the algebra and approximations is to simply use the Rayleigh-Sommerfeld diffraction integral of the first kind (RS1) as given in equation (1) and finding the electric field by numerical integration using Simpson's rule.

Figure (1) shows a simple arrangement for the focusing of a point source by a lens. The image is also just a point. We can discuss the electric field from a single point and then obtain the electric field distribution at the image by a coherent superposition of all the point sources. The object distance d_1 , the image distance d_2 and the focal length of the lens f are connected by the thin lens equation

$$\frac{1}{d_1} + \frac{1}{d_2} = \frac{1}{f}$$

A focused beam of monochromatic radiation (wavelength λ and propagation constant $k = 2\pi/\lambda$) from a lens is modelled by considering the convergence of spherical waves to the geometrical focus of the lens. If the point source is located at an infinite from the aperture, then the focal plane and image plane coincide and the image is formed in the focal plane.

$$d_1 \rightarrow \infty \quad \frac{1}{d_1} \rightarrow 0 \quad d_2 \rightarrow f$$

For the point source where $d_1 \rightarrow \infty$, we replace the focussing action of the lens by considering the convergence of spherical wavefronts from a circular aperture to a focus point at the position of the focal plane. The point source $S(x_S, y_S, z_S)$ is now located at the geometrical focus of the converging spherical waves and at a distance r_{OS} from the origin O located at the centre of the aperture as shown in figures (2) and (3).

The electric field E_Q of strength E_S at an aperture point $Q(x_Q, y_Q, 0)$ at a distance r_{QS} from the source point S is given by

$$(4) \quad E_Q(x_Q, y_Q, 0) = \frac{E_S \exp(-jk r_{QS})}{r_{QS}}$$

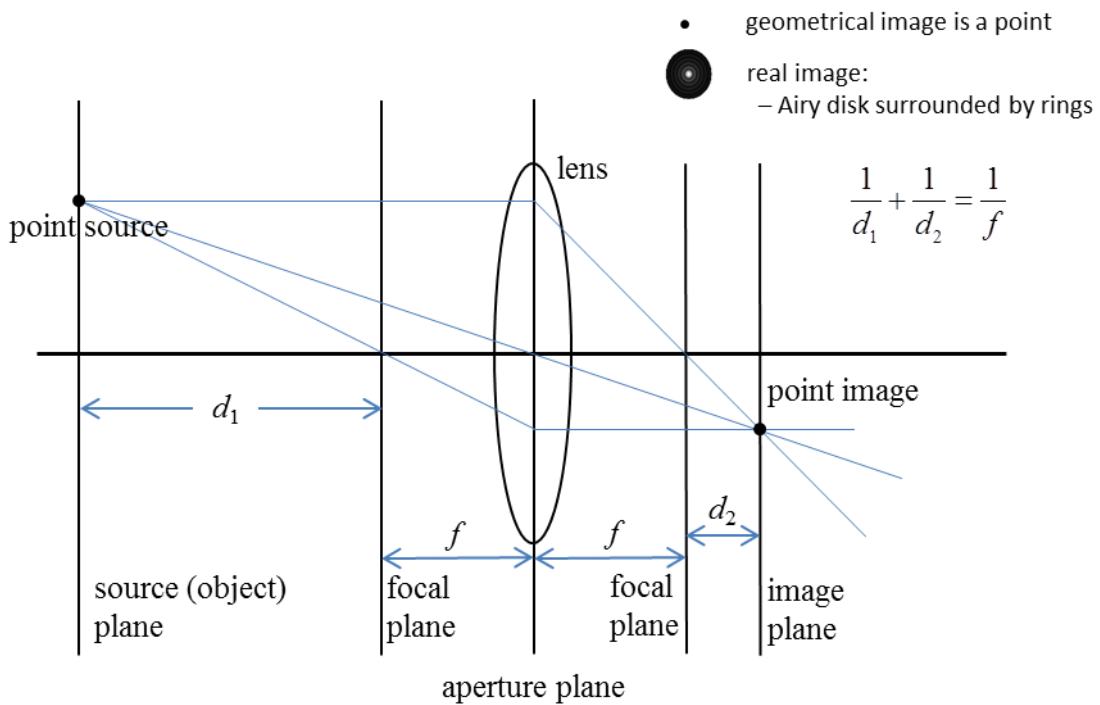


Fig. 1. Gaussian optical system for the focussing action of a lens for a point source.

For spherical waves shown in figure (2), the radiant flux would always be confined to a cone and so the radiant flux density would be infinite at the focus point. This can't happen, the energy carried by the wave must spread so the focal point must have some finite size. This phenomenon is called diffraction, that is, diffraction results from the limitations of the size of the wave surface emerging through the finite exit pupil of the aperture. Also, aberrations reduce the central radiant flux density with more energy being in the outer rings and the diffraction pattern may no longer be symmetrical about the optical axis, hence, aberrations cause a further spreading of the image of the point source. The total image field plane is a superposition of all the individual diffraction patterns when the proper accounting is done for the relative phases.

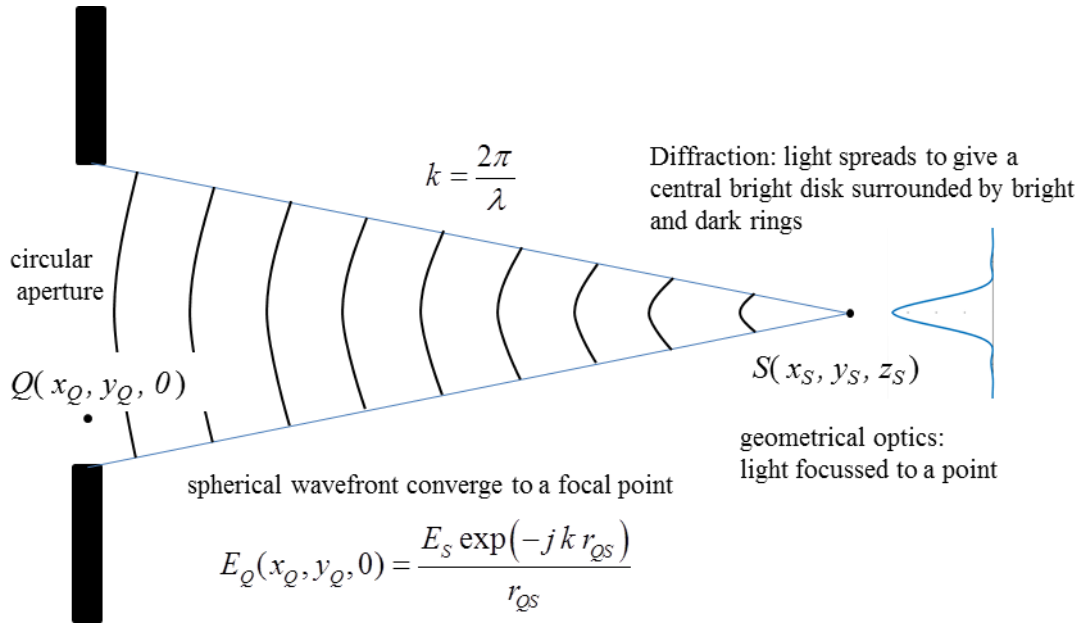


Fig. 2. Spherical waves from a circular aperture converge to a focal point.

The electric field E_P at a point $P(x_P, y_P, z_P)$ in the image space is calculated from the RS1 diffraction integral given by equation (5)

$$(5) \quad E_P(x_P, y_P, z_P) = \frac{1}{2\pi} \iint_{S_A} \frac{T E_S \exp(-jk r_{QS})}{r_{QS}} \frac{\exp(jk r_{QP})}{r_{QP}^3} z_p (jk r_{QP} - 1) dS$$

where r_{QS} is the distance from an aperture point Q to the source point S and r_{QP} is the distance from the aperture point Q to an observation point P . The term T is the transmission function for a filter to modify the electric field within the pupil or an aberration factor of the form $\exp(-jk \Delta)$ where Δ is a function of the optical path differences between the spherical wavefront emerging from the aperture and the aberrated wavefront. If there is no mask or zero aberration effects then $T = 1$. The geometry for the calculation is shown in figure (3).

The three-dimensional radiant flux density (irradiance) in the vicinity of the focal region is calculated from equation (2)

$$(2) \quad w_e = \frac{n \epsilon_0 c}{2} E_P^* E_P$$

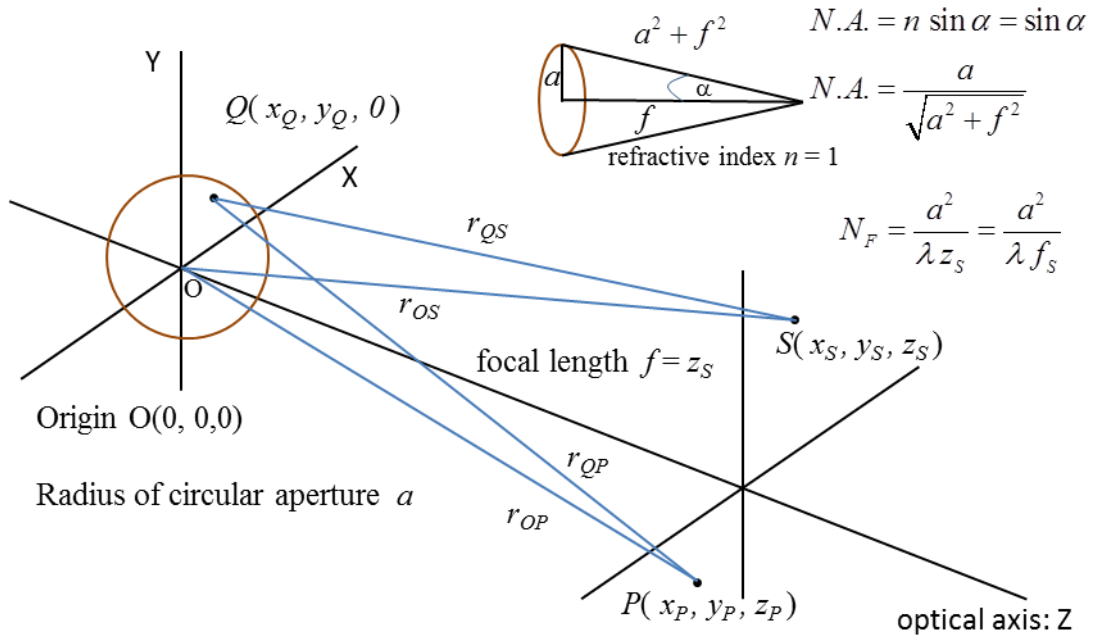


Fig. 3. Geometry for the calculation of E_P for the spherical waves emitted from the circular aperture to the focal point S.

The numerical aperture $N.A.$ of an optical system is a dimensionless number that characterizes the range of angles over which the system can accept or emit light (figure 3). In most areas of optics, and especially in microscopy, the numerical aperture of an optical system such as an objective lens is defined by

$$(6) \quad N.A. = n \sin \alpha = \sin \alpha = \frac{a}{\sqrt{a^2 + f^2}}$$

where the refractive index is $n = 1$ will only be considered and α is the half-aperture angle of the maximum cone of light that can enter or exit the lens. In general, this is the angle of the real marginal ray in the system. Most approximation methods for calculating the irradiance in the focal region assume that the numerical aperture $N.A.$ is small and the radius of the aperture is much greater than the wavelength

$$(7) \quad (N.A.)^2 \ll 1 \quad \text{or} \quad a^2/f^2 \ll 1 \quad \text{and} \quad a \gg \lambda$$

By the direct numerical integration of diffraction integrals, these limitations are not so restrictive.

The irradiance in the focal region depends upon the wavelength λ , aperture radius a , and the focal distance $f = z_S$. To characterize the focusing geometry, the Fresnel number N_F is defined by

$$(8) \quad N_F = \frac{a^2}{\lambda z_S}$$

The Fresnel number can be thought of as the number of Fresnel zones that fill the aperture when the aperture is viewed from the geometrical focus. The wave field near the geometrical focus region depends upon the Fresnel number.

For calculating the irradiance it is useful to define two optical coordinates for the axial and radial directions

$$(9) \quad u_p = \frac{k a^2}{z_S} (z_p - z_S) \quad \text{axial optical coordinate}$$

$$(10) \quad v_p = \frac{k a}{z_S} x_p \quad \text{radial optical coordinate}$$

For low numerical apertures $(N.A.)^2 \ll 1$, the Fresnel number N_F is an excellent parameter in describing the structure of the focal region. Low $N.A.$ focusing system corresponds to the Fraunhofer region and it can be shown that the axial and radial irradiance distributions are described by simple analytical expressions

$$(11) \quad I(u_p, 0) = I_{\max} \left(\frac{\sin(u_p/4)}{(u_p/4)} \right)^2 \quad \text{axial irradiance}$$

$$(12) \quad I(0, v_p) = I_{\max} \left(\frac{2 J_1(v_p)}{v_p} \right)^2 \quad \text{radial irradiance}$$

Equations (11) and (12) can be derived from the Fresnel-Kirchhoff diffraction integral using the Debye parabolic approximation where spherical wavefronts are replaced by paraboloids in paraxial systems. Equations (11) and (12) imply that in the neighbourhood of the focal region, the irradiance distribution is symmetrical about the focal plane with the maximum irradiance occurring at the geometrical focus.

The zeros along the optical axis occur at

$$(13) \quad u_P / 4\pi = 1, 2, 3, \dots$$

The irradiance distribution in the focal plane is the familiar Airy disk pattern where J_1 is the Bessel function of the first kind and the zeros in the radial direction occur at

$$(14) \quad v_P / \pi = 1.220, 2.233, 3.238, \dots$$

Equations (11) to (14) describe the Fraunhofer diffraction in the focal region.

AXIAL IRRADIANCE DISTRIBUTION

The irradiance distribution along the optical axis in a region near the focal plane at $z = z_S$ is calculated numerically using the mscript `op_rs_fb_z.m` for optical systems with different Fresnel numbers.

Simulation 1: Large Fresnel Number $N_F = 1580$

Table 1 gives a summary of the input parameters used in the simulation. The execution time for the mscript was about 10 seconds.

Table 1. Input parameters for $N_F = 1580$

wavelength $\lambda = 6.328 \times 10^{-7}$ m

Partitions

inner ring $n_1 = 201$

outer inner ring $n_2 = 801$

rings $n_R = 201$

$n_Q = 101003$

$n_P = 509$

Source

$x_S = 0$ m

$y_S = 0$ m

$z_S = 0.100$ m

focal length $f = 0.100$ m

Aperture space

radius of aperture $a = 0.010$ m

Fresnel Number $N_F = 1580$

Numerical Aperture $N.A. = 0.100$

Observation space P

max distance from focal plane $|z_P - z_S|_{\max} = 0.850 \times 10^{-3}$ m

Figures (4) and (5) show the graphical output for the variation in irradiance along the optical axis. Tables 2 gives a summary of the positions of the zeros in the irradiance distribution and Table 3 a summary of the positions of the peaks and their relative strengths.

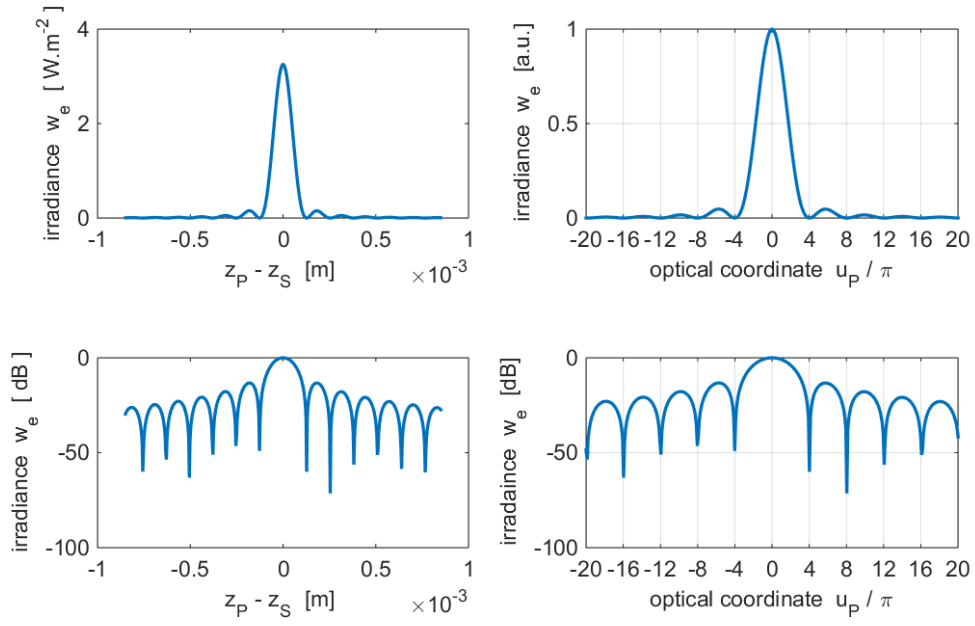


Fig. 4. The axial irradiance near the focal point.

$$\lambda = 632.8 \text{ nm} \quad a = 0.01 \text{ m} \quad f = 0.1 \text{ m} \quad N_F = 1580 \quad N.A. = 0.10$$

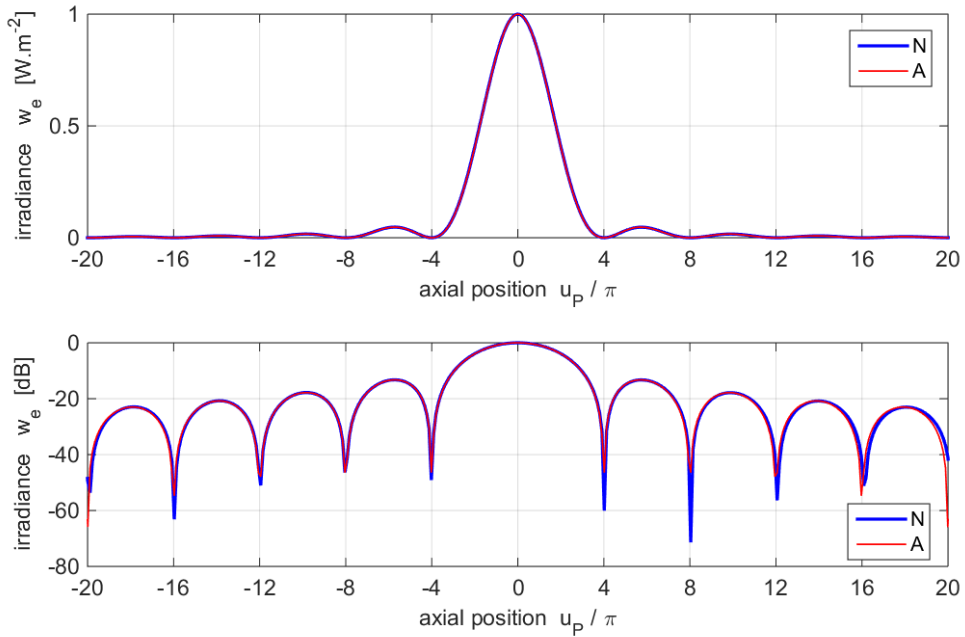


Fig. 5. The axial irradiance near the focal point.

The blue curve is the numerical calculation (N) and the red curve (A) is calculated using equation (11).

$$\lambda = 632.8 \text{ nm} \quad a = 0.01 \text{ m} \quad f = 0.1 \text{ m} \quad N_F = 1580 \quad N.A. = 0.10$$

The msript **turningPoint.m** can be used to find the positions of the zero and positions and values of the peaks in the irradiance distribution.

Table 2: Zeros* in the irradiance distribution

	N RS1 Numerical calculation					A Analytical calculation (equation 11)			
N	-15.97	-11.95	-8.04	-4.02	4.02	8.04	12.06	16.08	
A	-15.97	-11.95	-8.04	-4.02	4.02	8.04	11.95	15.97	

* The slight discrepancies in the values compared with the exact values of $\pm 4, \pm 8, \pm 12, \dots$ is due to the partitioning of the Z axis in the calculations: grid spacing $\Delta z_P = 3.35 \times 10^{-6}$ m and $\Delta u_P = 0.1$.

Table 3: Positions and relative values for the peak in the irradiance distribution

	N RS1 Numerical calculation					A Analytical calculation (equation 11)				
N u_P	-17.88	-13.86	-9.84	-5.71	0	5.71	9.94	13.96	18.09	
N peaks	0.0051	0.0084	0.0166	0.0474	1.000	0.0470	0.0164	0.0083	0.0050	
A u_P	-17.88	-13.86	-9.84	-5.71	0	5.71	9.84	13.86	17.88	
A peaks	0.0050	0.0083	0.0165	0.0472	1.000	0.0472	0.0165	0.0083	0.0050	

The figures (4) and (5) and the results given in Tables 2 and 3 clearly demonstrate the excellent agreement between the numerical computation of RS1 diffraction integral and the predictions using the Debye approximation ($a \gg \lambda$ and $a^2 / \lambda f \gg 1$ or Fresnel number $N_F \gg 1$). The irradiance distribution is characteristic of the Fraunhofer pattern and is symmetrical about the focal point.

Simulation 2: Intermediate Fresnel Number $N_F = 316$

Table 4 gives a summary of the input parameters used in the simulation. The execution time for the msript was about 10 seconds. The only changes to the parameters used in Simulation 1 were the focal length f or axial position of the source z_S and the range of z_P values. The focal length f was increased from 0.1 m to 0.5 m to reduce the value of the Fresnel number N_F .

Table 4. Input parameters for $N_F = 316$

$$\text{wavelength } \lambda = 6.328 \times 10^{-7} \text{ m}$$

Partitions

$$\text{inner ring } n_1 = 201$$

$$\text{outer inner ring } n_2 = 801$$

$$\text{rings } n_R = 201$$

$$n_Q = 101003$$

$$n_P = 509$$

Source S

$$x_S = 0 \text{ m}$$

$$y_S = 0 \text{ m}$$

$$z_S = 0.500 \text{ m}$$

$$\text{focal length } f = 0.500 \text{ m}$$

Aperture space Q

$$\text{radius of aperture } a = 0.010 \text{ m}$$

$$\text{Fresnel Number } N_F = 1580$$

$$\text{Numerical Aperture } N.A. = 0.020$$

Observation space P

$$\text{max distance from focal plane } |z_P - z_S|_{\max} = 0.018 \text{ m}$$

Figures (6) and (7) show the graphical output for the variation in irradiance along the optical axis. Tables 5 gives a summary of the positions of the zeros in the irradiance distribution and Table 6 a summary of the positions of the peaks and their relative strengths.

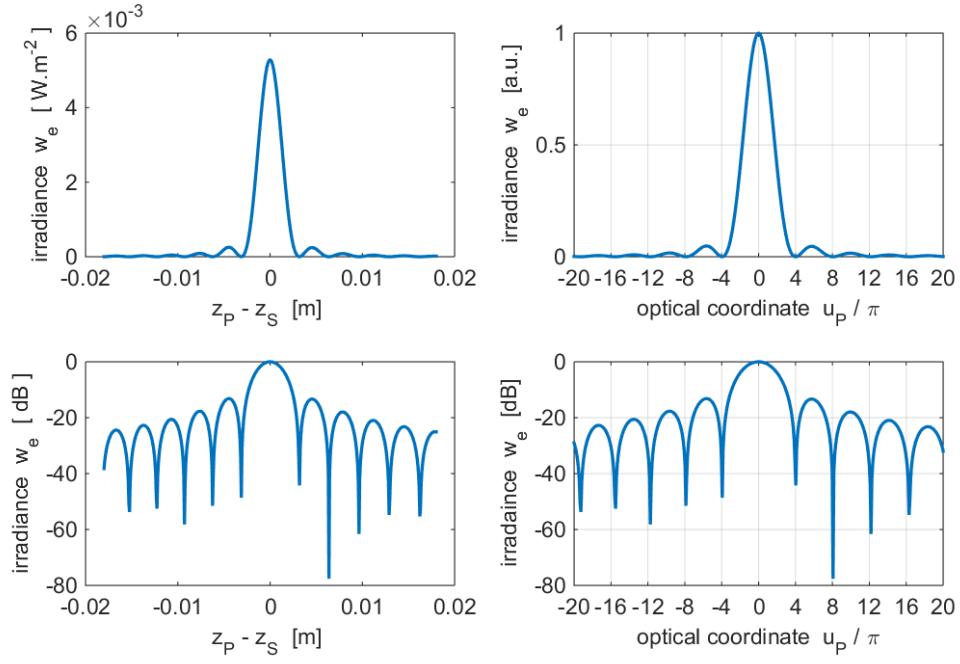


Fig. 6. The axial irradiance near the focal point.

$$\lambda = 632.8 \text{ nm} \quad a = 0.01 \text{ m} \quad f = 0.5 \text{ m} \quad N_F = 316 \quad N.A. = 0.020$$

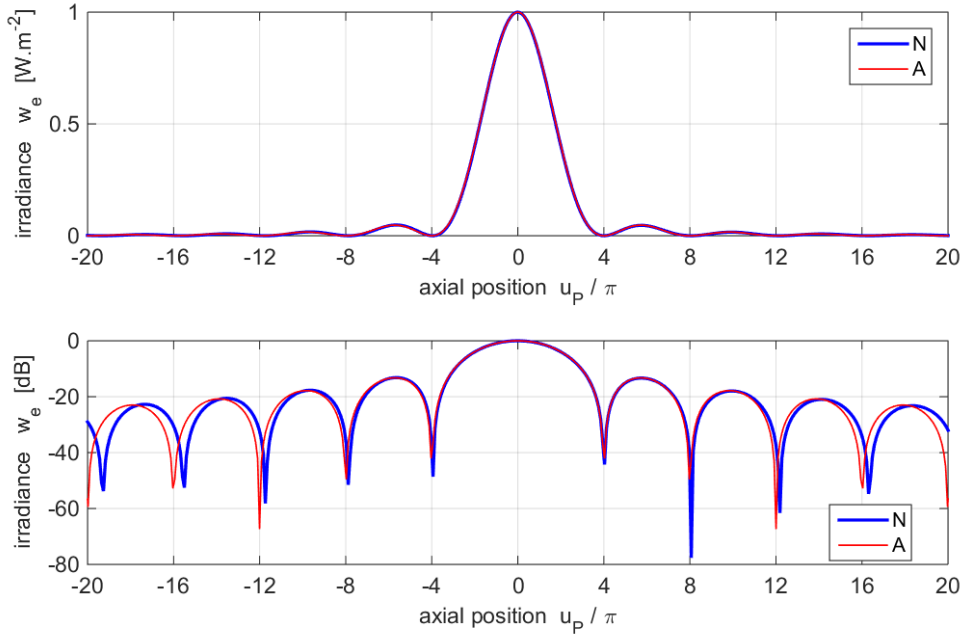


Fig. 7. The axial irradiance near the focal point.

The blue curve is the numerical calculation (N) and the red curve (A) is calculated using equation (11).

$$\lambda = 632.8 \text{ nm} \quad a = 0.01 \text{ m} \quad f = 0.5 \text{ m} \quad N_F = 316 \quad N.A. = 0.020$$

The msript **turningPoint.m** can be used to find the positions of the zero and positions and values of the peaks in the irradiance distribution.

Table 5: Zeros* in the irradiance distribution

	N RS1 Numerical calculation				A Analytical calculation (equation 11)			
N	-15.50	-11.74	-7.88	-3.94	4.03	8.06	12.18	16.31
A	-16.04	-12.01	-7.97	-4.03	4.03	7.97	12.01	16.04

* The slight discrepancies in the values compared with the exact values of $\pm 4, \pm 8, \pm 12, \dots$ is due to the partitioning of the Z axis in the calculations: grid spacing $\Delta z_P = 3.35 \times 10^{-6}$ m and $\Delta u_P = 0.1$.

Table 6: Positions and relative values for the peak in the irradiance distribution

	N RS1 Numerical calculation				A Analytical calculation (equation 11)				
N u_P	-17.38	-13.53	-9.68	-5.64	0	5.73	9.95	14.16	18.37
N peaks	0.0053	0.0087	0.0170	0.0481	1.000	0.0464	0.0160	0.0080	0.0048
A u_P	-17.92	-13.89	-9.86	-5.73	0	5.73	9.86	13.89	17.92
A peaks	0.0050	0.0083	0.0165	0.0472	1.000	0.0472	0.0165	0.0083	0.0050

The figures (6) and (7) and the results given in Tables 5 and 6 only demonstrate a reasonable agreement between the numerical computation of RS1 diffraction integral and the predictions using the Debye approximation. The irradiance distribution is slightly asymmetrical about the focal plane. For positive u_P values, the pattern is slightly stretched as that the zero and peaks occur at larger u_P values than for the parameters used in Simulation 1 (large Fresnel number). For negative u_P values, the pattern is slightly compressed as that the zero and peaks occur at smaller $|u_P|$ values than for the parameters used in Simulation 1 (large Fresnel number).

The Fresnel number could have been reduced by decreasing the radius of the aperture or increasing the wavelength instead of the focal length. The irradiance plotted against the axial optical coordinate as shown in figures (6) and (7) depend upon the value of the Fresnel number and the plots are roughly independent on the values used for the wavelength, aperture radius or focal length. The irradiance patterns are insensitive to changes in wavelength, aperture radius or focal length when plotted in terms of the optical coordinates. Therefore, the Fresnel number is an excellent parameter for describing the structure of the irradiance distribution in the focal region.

Simulation 3: Small Fresnel Number $N_F = 15.80$

Table 7 gives a summary of the input parameters used in the simulation. The execution time for the msript was about 50 seconds. The only changes to the parameters used in Simulation 1 were the focal length f or axial position of the source z_S and the range of z_P values. The focal length f was increased from 0.100 m to 10.0 m to reduce the value of the Fresnel number N_F . The number of partitions of the optical axis n_P has to be larger than in Simulation 1 because of the more rapid variation in the irradiance distribution.

Table 7. Input parameters for $N_F = 15.80$

wavelength $\lambda = 6.328 \times 10^{-7}$ m

Partitions

inner ring $n_1 = 201$

outer inner ring $n_2 = 801$

rings $n_R = 201$

$n_Q = 101003$

$n_P = 1509$

Source S

$x_S = 0$ m

$y_S = 0$ m

$z_S = 10.00$ m

focal length $f = 10.00$ m

Aperture space Q

radius of aperture $a = 0.010$ m

Fresnel Number $N_F = 15.80$

Numerical Aperture $N.A. = 0.0010$

Observation space P

max distance from focal plane $|z_P - z_S|_{\max} = 5.00$ m

Figures (6) and (7) show the graphical output for the variation in irradiance along the optical axis. Tables 8 gives a summary of the positions of the zeros in the irradiance distribution and Table 9 a summary of the positions of the peaks and their relative strengths.

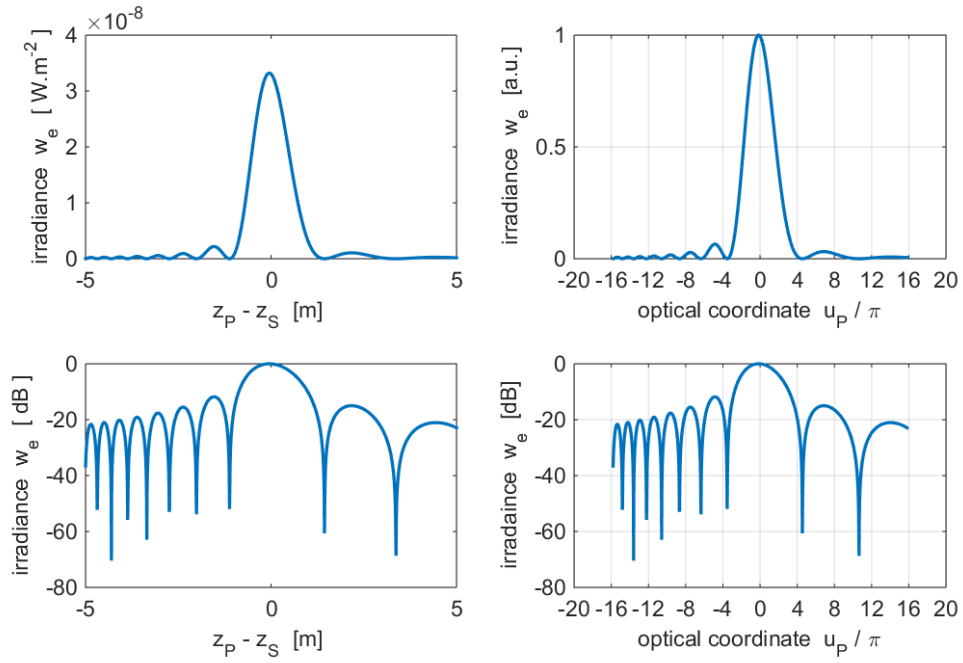


Fig. 8. The axial irradiance near the focal point.

$$\lambda = 632.8 \text{ nm} \quad a = 0.01 \text{ m} \quad f = 10.0 \text{ m} \quad N_F = 15.8 \quad N.A. = 0.001$$

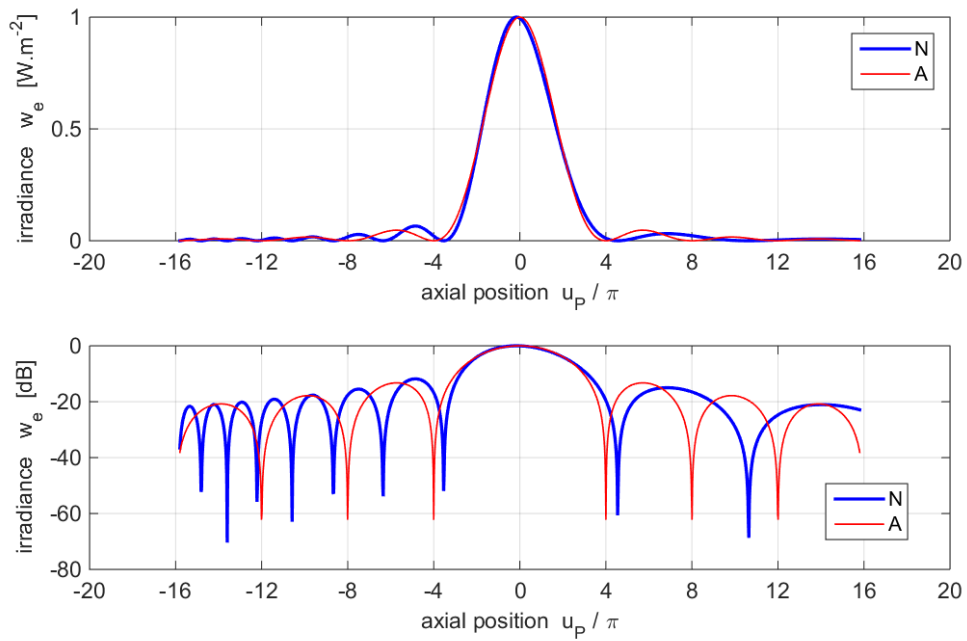


Fig. 9. The axial irradiance near the focal point.

The blue curve is the numerical calculation (N) and the red curve (A) is calculated using equation (11).

$$\lambda = 632.8 \text{ nm} \quad a = 0.01 \text{ m} \quad f = 10.0 \text{ m} \quad N_F = 15.8 \quad N.A. = 0.0010$$

The mscript **turningPoint.m** can be used to find the positions of the zero and positions and values of the peaks in the irradiance distribution.

Table 8: Zeros* in the irradiance distribution

N RS1 Numerical calculation

N	-14.82	-13.60	-12.22	-10.58	-8.66	-6.35	-3.54	4.55	10.65
----------	--------	--------	--------	--------	-------	-------	-------	------	-------

Table 9: Positions and relative values for the peak in the irradiance distribution

N RS1 Numerical calculation

N u_P	-14.21	-12.91	-11.40	-9.62	-7.50	-4.86	-0.147	6.85	14.02
N peaks	0.0080	0.0096	0.0123	0.0172	0.0282	0.0655	1.0000	0.0317	0.0078

The figures (8) and (9) and the results given in Tables 8 and 9 demonstrates that there is **no** agreement between the numerical computation of RS1 diffraction integral and the predictions using the Debye approximation. The irradiance distribution is now asymmetrical about the focal plane with the central peak not occurring at the focal plane but the position is shifted towards the aperture at $u_P = -0.147$. For positive u_P values, the pattern is slightly stretched as that the zero and peaks occur at larger u_P values than for the parameters used in Simulation 1 (large Fresnel number). For negative u_P values, the pattern is highly compressed as that the zero and peaks occur at smaller $|u_P|$ values than for the parameters used in Simulation 1.

IRRADIANCE IN THE MERIDIONAL PLANE

Simulation 4 `op_rs_fb_xz.m`

The irradiance in the meridional plane (XZ plane) is shown in figures 10 to 12 when the source point for the converging spherical waves is located on the optical axis. The irradiance contours are shown for the region near the focal point. The irradiance is given in decibels $w_e(\text{dB}) = 10 \log_{10}(w_e / w_{e\text{max}})$. The u_P values represent scaled distance from the source point along the optical axis and the v_P values represent scaled distances from the optical axis in the observation plane. The back lines show the geometrical shadow region.

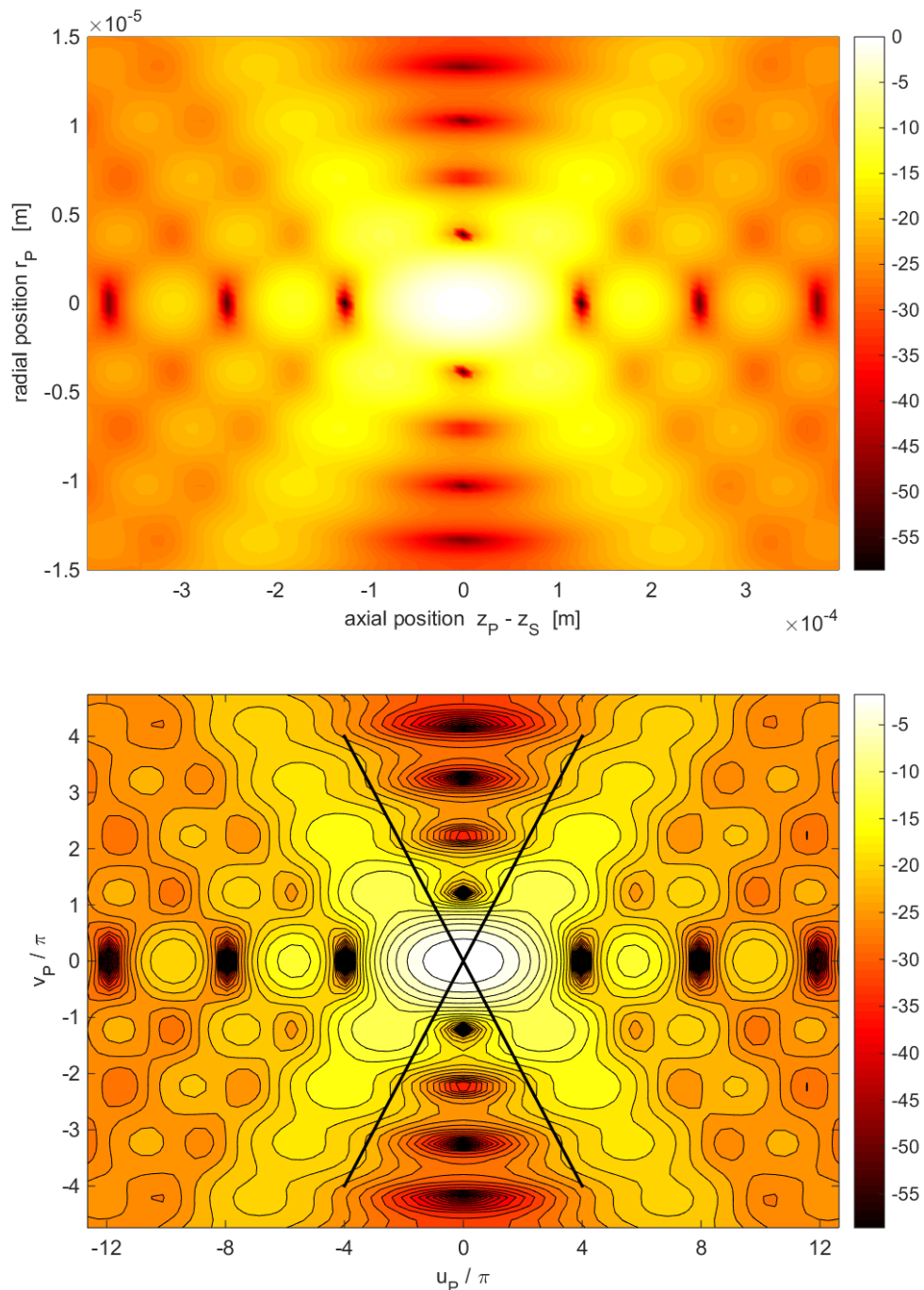


Fig. 10. Irradiance (dB) in the meridional plane for high Fresnel number.

$\lambda = 632.8 \text{ nm}$ $a = 0.01 \text{ m}$ $S(0, 0, 0.1 \text{ m})$ $f = 0.1 \text{ m}$ $N_F = 1580$ $N.A. = 0.1$

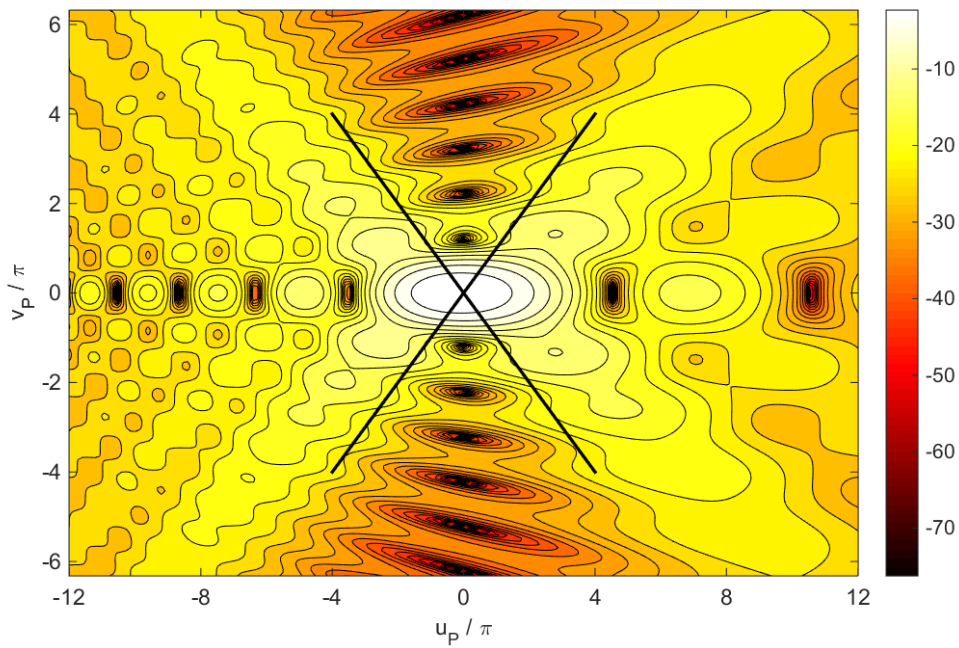
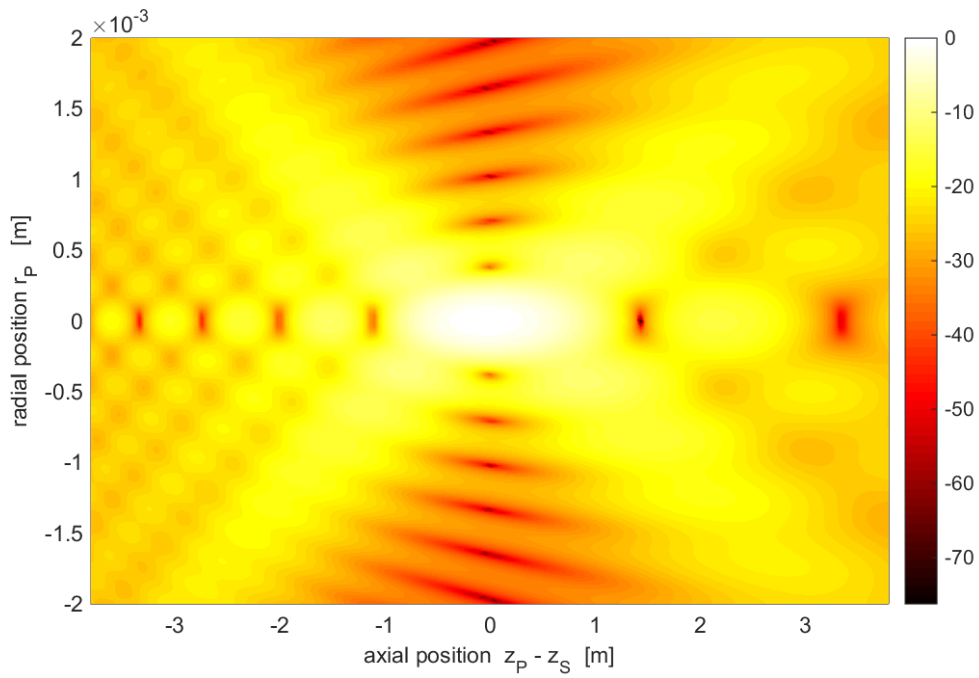


Fig. 11. Irradiance (dB) in the meridional plane for low Fresnel number.
 $\lambda = 632.8 \text{ nm}$ $a = 0.01 \text{ m}$ $S(0, 0, 10 \text{ m})$ $f = 10 \text{ m}$ $N_F = 15.80$ $N.A. = 0.0010$

For the low Fresnel number case, the irradiance distribution is not symmetrical about the image plane ($u_p = 0$) and the maximum in the irradiance is shifted slightly towards the aperture.

IRRADIANCE IN AN OBSERVATION PLANE

The mscript `op_rs_fb_xy.m` can be used to calculate the irradiance pattern in an XY observation plane only when the irradiance distribution is circularly symmetric about the optical Z axis. When the observation plane coincides with the focal plane and the Fresnel number is large, the irradiance pattern in a radial direction calculated numerical from the RS1 diffraction integral (equation 5) agrees with the prediction of the Debye approximation of the diffraction integral given by equation (12) as shown by the results given in Simulation 5. However, for small Fresnel numbers as in Simulation 6, the Debye predictions of the irradiance pattern are no longer valid. For Simulations 5 and 6, the observation plane coincides with the focal plane ($f = z_S = z_P$).

Simulation 5 Irradiance in the focal (image) plane

Table 10. Parameters for large Fresnel number (execution time ~ 35 seconds)

wavelength $\lambda = 632.8$ nmm

Partitions

inner ring $n_1 = 201$

outer inner ring $n_2 = 801$

rings $n_R = 285$

$n_Q = 143075$

$n_P = 1285$

Source (source must be on the optical axis in using `op_rs_fb_xy1.m`)

$x_S = 0$ m

$y_S = 0$ m

$z_S = 0.100$ m

focal length $f = 0.100$ m

$E_S = 1.00 \times 10^{-3}$ V.m⁻¹

Aperture space

radius of aperture $a = 0.010$ m

max irradiance $w_{eQ} = 1.314 \times 10^{-7}$ W.m⁻²

radiant flux max irradiance $W_{EQ} = 4.163 \times 10^{-11}$ W

Fresnel Number $N_F = 1580$

Numerical Aperture $N.A. = 0.100$

Observation space

max radius $r_P = 1.980 \times 10^{-5}$ m

distance aperture to observation plane $z_P = 0.10$ m

max irradiance $w_{max} = 3.245$ W.m⁻²

radiant flux $W_E = 4.026 \times 10^{-11}$ W

% radiant flux enclosed within 1st min = 83.7

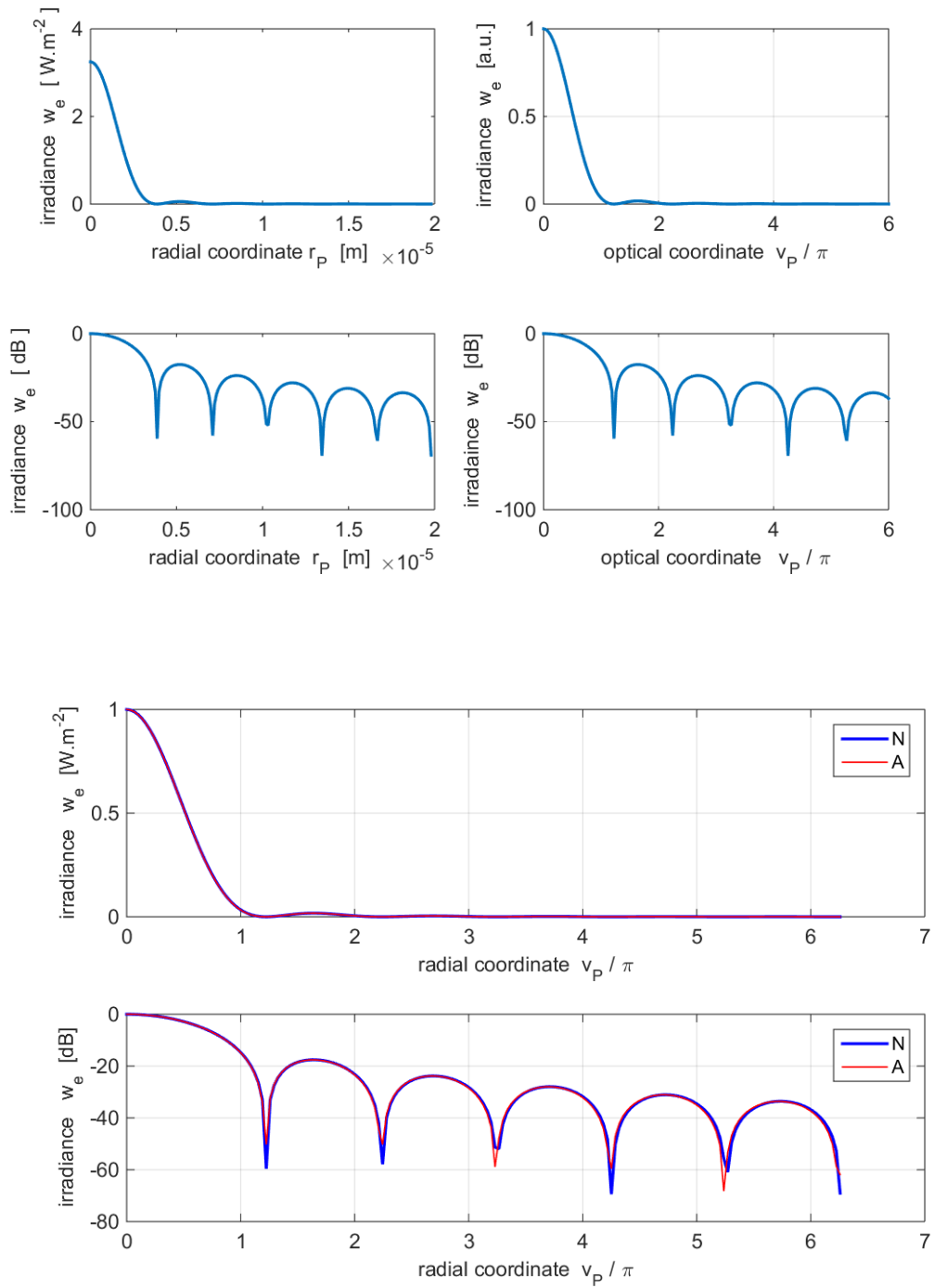


Fig. 12. The radial irradiance in the focal plane. The blue curve is the RS1 numerical calculation (N) and the red curve (A) is calculated using equation (12).

$$\lambda = 632.8 \text{ nm} \quad a = 0.01 \text{ m} \quad f = 0.100 \text{ m} \quad N_F = 1580 \quad N.A. = 0.100$$

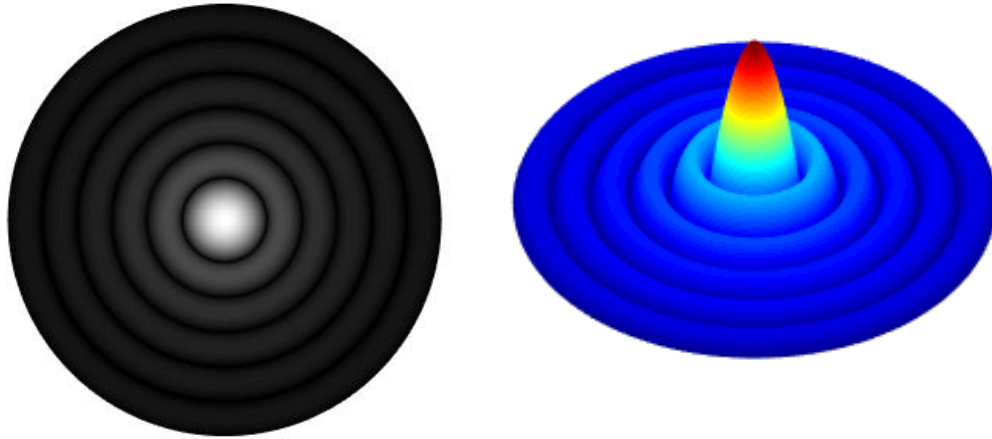


Fig. 13. Irradiance (dB) distribution on the focal plane.

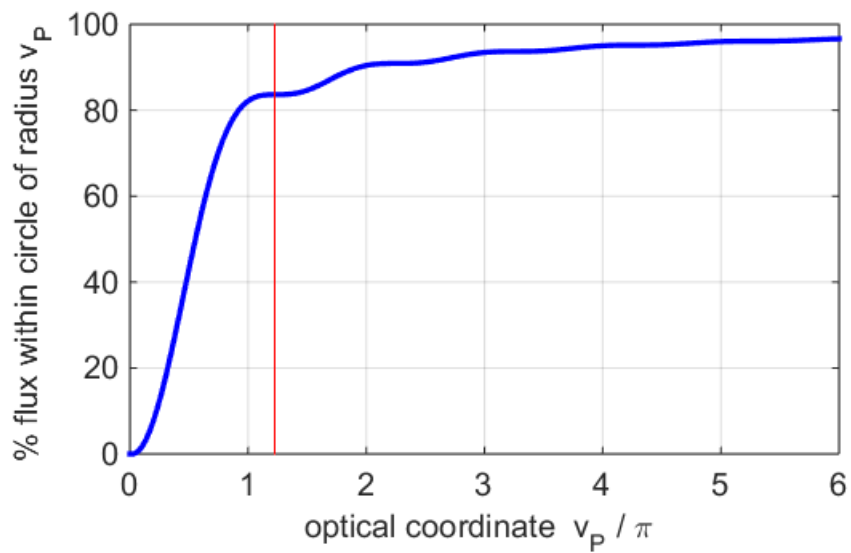


Fig. 14. Percentage of energy enclosed within a circle of prescribed radius. The red vertical line shows the position of the first minimum in the diffraction pattern.

The msript **turningPoint.m** can be used to find the positions of the zero and positions and values of the peaks in the irradiance distribution.

Table 11. v_P / π zeros in the irradiance distribution

N RS1 Numerical calculation **A** Analytical calculation (equation 12)

N	1.22	2.24	3.25	4.26	5.26
A	1.22	2.23	3.24	4.24	5.24

* uncertainty $\Delta v_P = 0.01$

Table 12. Positions v_P/π and relative values for the peak in the irradiance distribution

N RS1 Numerical calculation **A** Analytical calculation (equation 12)

N u_P	1.64	2.69	3.71	4.72	5.74
N peaks	0.0176	0.0042	0.0016	0.0008	0.0004
A u_P	1.63	2.68	3.70	4.71	5.72
A peaks	0.0175	0.0042	0.0016	0.0008	0.0004

* uncertainty $\Delta v_P = 0.01$

The figure (12) and the results given in Tables 11 and 12 clearly shows the excellent agreement between the numerical computation of the RS1 diffraction integral and the predictions using the Debye approximation.

The irradiance distribution has a central bright spot called the Airy disk and it is surrounded by circular bright rings of rapidly decreasing strength which are separated by dark rings as shown in figure (13).

Figure (14) shows the radiant flux enclosed with circles of increasing radius in the observation plane. The radiant flux emitted from the aperture pupil must equal the radiant flux through the observation plane because of conservation of energy. By the focussing action of the optical system modelled, most of the energy is concentrated into the Airy disk with 84% of the radiant flux within the first dark ring.

Changing the Fresnel number to $N_F = 15.80$ by increasing the focal length to $f = 10.00$ m does not change the irradiance distribution as a function of the radial coordinate v_P . However, the radius of the Airy disk expressed in meters is much larger as shown in figure (15) as compared to figure (12).

The location of the first minimum:

$$\begin{array}{ll}
 N_F = 1580 & r_P(1^{\text{st}} \text{ min}) = 3.9 \times 10^{-6} \text{ m} \\
 N_F = 15.80 & r_P(1^{\text{st}} \text{ min}) = 3.9 \times 10^{-4} \text{ m}
 \end{array}$$

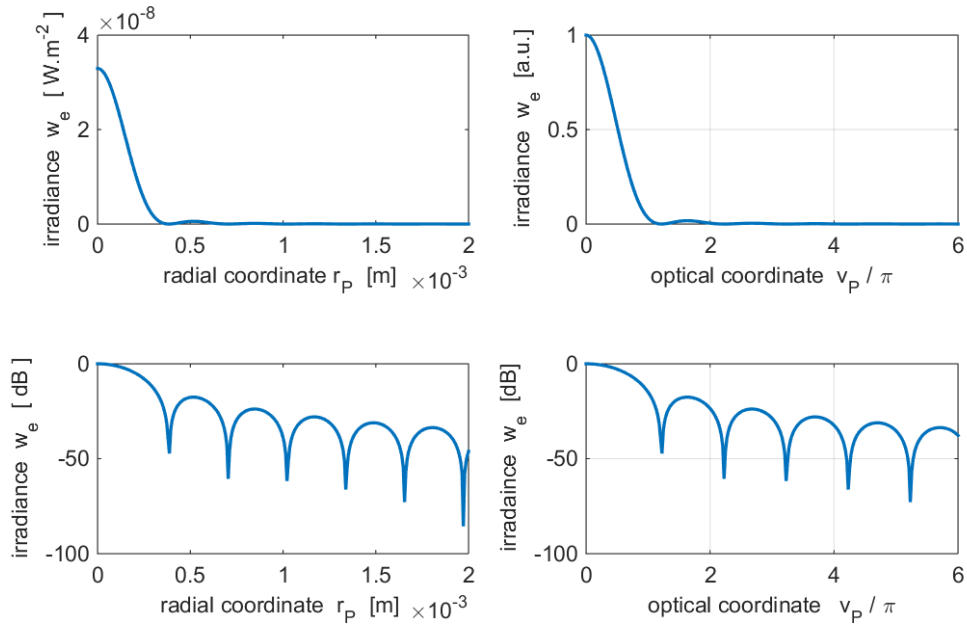


Fig. 14. The radial irradiance in the focal plane.

$$\lambda = 632.8 \text{ nm} \quad a = 0.01 \text{ m} \quad f = 10.00 \text{ m} \quad N_F = 15.80 \quad N.A. = 0.100$$

Simulation 6 Irradiance in a non-focal plane

For Simulation 6, the parameters used were the same as in Simulation 5 except the observation plane was closer to the aperture than the focal plane

$$\text{focal plane} \quad f = 0.0100 \text{ m}$$

$$\text{observation plane} \quad z_P = f - 5 \times 10^{-5} \text{ m} = 0.09950 \text{ m}$$

The irradiance distribution is no longer that of a Fraunhofer diffraction pattern. There are no clear zeros in the diffraction pattern.

Simulation 5 focal plane Fraunhofer diffraction	Simulation 6 non-focal plane Fresnel diffraction
Max irradiance 3.2 W.m^{-2}	max irradiance 1.9 W.m^{-2}
Radiant flux within 1 st min Fraunhofer pattern ($v_P = 1.22\pi$) = 84 %	Radiant flux within 1 st min Fraunhofer pattern ($v_P = 1.22\pi$) = 60 %

The graphical output for Simulation 6 is shown in figures (15) and (16).

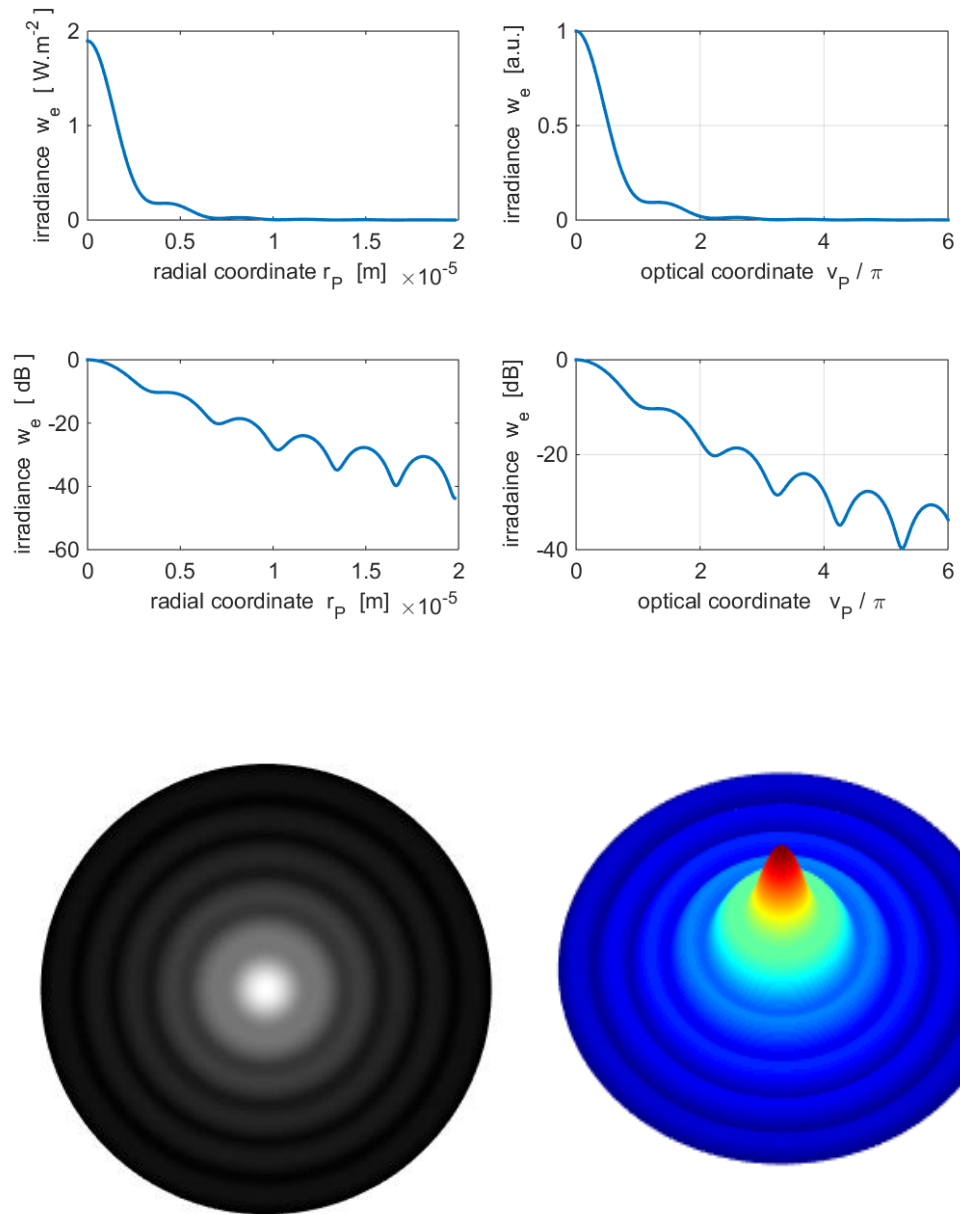


Fig. 15. The radial irradiance in a non-focal plane .

$$\lambda = 632.8 \text{ nm} \quad a = 0.01 \text{ m} \quad f = 0.100 \text{ m} \quad N_F = 1580 \quad N.A. = 0.100$$

$$z_P = f - 5 \times 10^{-5} \text{ m} = 0.09950 \text{ m}$$

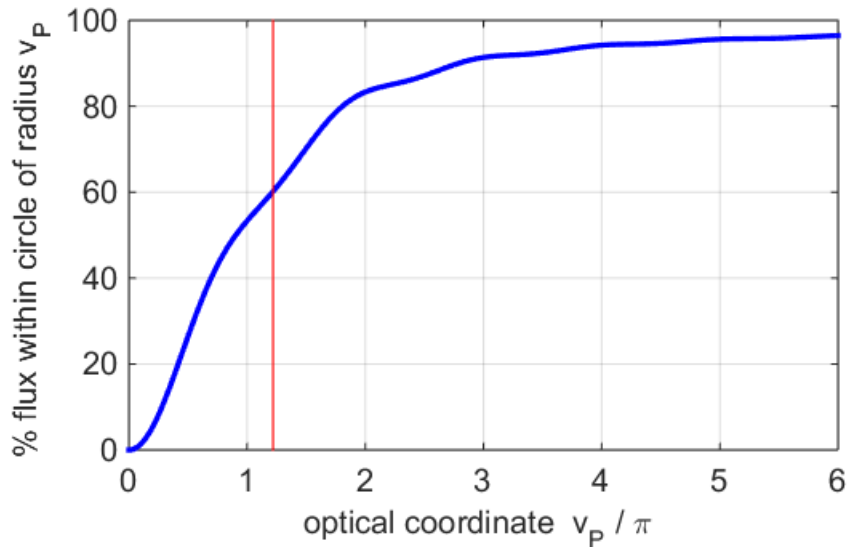


Fig. 16. Percentage of energy enclosed within a circle of prescribed radius. The red vertical line shows the position of the first minimum in the Fraunhofer diffraction pattern $v_p = 1.22\pi$.

Simulation 7

Irradiance in focal plane for an annular aperture

For Simulation 7, the parameters used were the same as in Simulation 5 except the integration is for an annular aperture where the limits of the integration are for $r_Q = a/2$ to a where a is the radius of the exit pupil.

The irradiance distribution is no longer that of a Fraunhofer diffraction pattern. There are no clear zeros in the diffraction pattern.

Simulation 5 circular aperture $r_Q = 0$ to a	Simulation 7 annular aperture $r_Q = a/2$ to a
Max irradiance 3.2 W.m^{-2}	max irradiance 1.8 W.m^{-2}
Radiant flux within 1 st min Fraunhofer pattern ($v_p = 1.22\pi$) = 84 %	Radiant flux within 1 st min Fraunhofer pattern ($v_p = 1.22\pi$) = 49 %
Position of 1 st min $v_p = 1.22\pi$	Position of 1 st min $v_p = 1.00\pi$

The graphical output for Simulation 7 is shown in figures (17) to (19). Although the central peak is narrower for the annular aperture compared with the full circular aperture, the maximum irradiance is much lower as more energy is concentrated in the outer side-lobes of the irradiance distribution.

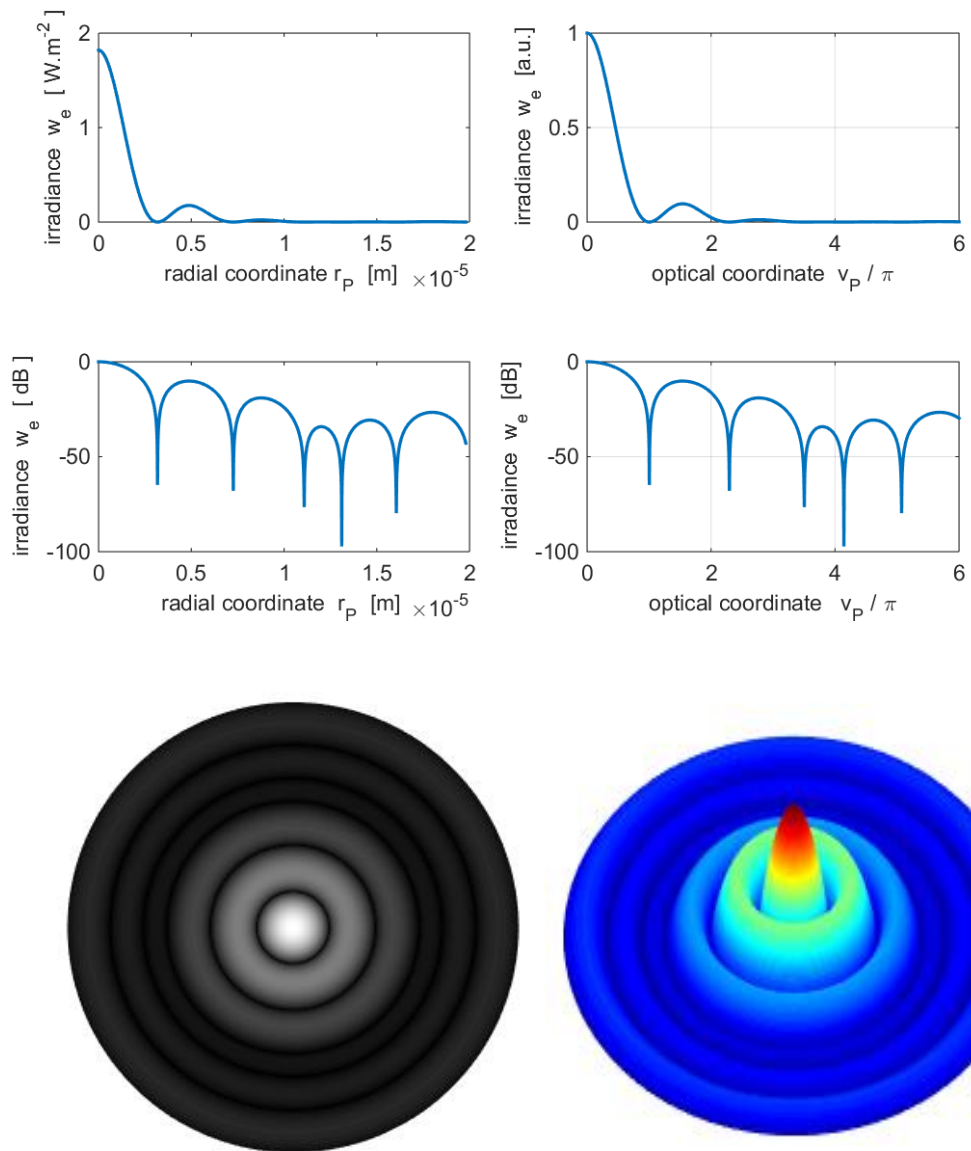


Fig. 17. The irradiance distribution for an annular aperture in the focal plane.
 $\lambda = 632.8 \text{ nm}$ $a = 0.01 \text{ m}$ $f = 0.100 \text{ m}$ $N_F = 1580$ $N.A. = 0.100$
 $r_Q = a/2$ to a

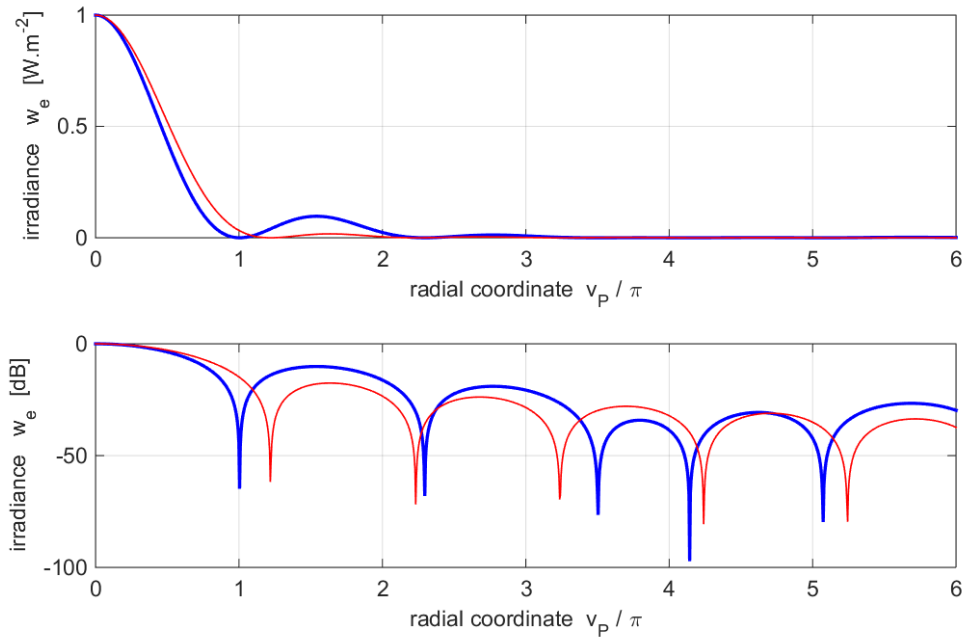


Fig 18. Irradiance distribution for the annular aperture (blue curves) compared with the full circular aperture (red curves).

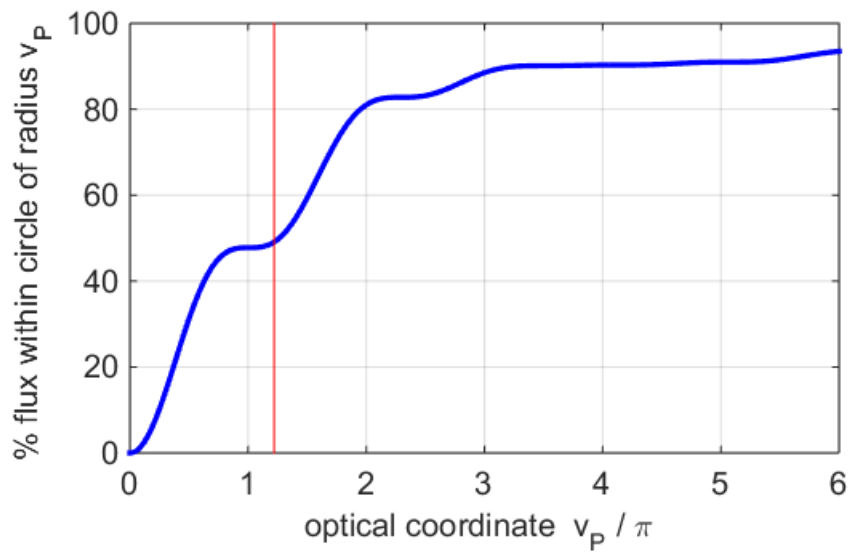


Fig. 19. Percentage of energy enclosed within a circle of prescribed radius. The red vertical line shows the position of the first minimum in the Fraunhofer diffraction pattern $v_p = 1.22\pi$.